

## AMBIGUITY AND DEPTH RESOLUTION IN POTENTIAL FIELD INVERSION

MAURIZIO FEDI

*Dipartimento di Scienze della Terra, Università degli Studi di Napoli "Federico II"  
Largo San Marcellino, 10, Naples, 80138, Italy  
E-mail: fedi@unina.it*

PER CHRISTIAN HANSEN

*Department of Informatics and Mathematical Modelling  
Technical University of Denmark, Building 321, DK-2800 Lyngby, Denmark  
E-mail: pch@imm.dtu.dk*

VALERIA PAOLETTI

*C.U.G.R.I., Viale Kennedy, 5, Naples, 80125, Italy  
E-mail: paoletti@unina.it*

### Abstract.

Inverse potential field problems have ambiguous solutions, and a unique solution can only be computed if additional a priori information is incorporated into the solution process. We discuss several kinds of ambiguity, and show how each type of ambiguity occurs and is handled differently. We demonstrate that potential-field data provide depth information when used in connection with certain discretizations of the problem, and that the role of the regularization term in the Tikhonov formulation is primarily to filter out noise. In addition we show how the inspection of two graphical tools, based on the singular value decomposition, can guide the regularization and also reveal how much depth information can be achieved for a given noisy problem.

*Keywords:* Inverse problems, potential field inversion, regularization, SVD analysis, ambiguity, depth resolution.

### 1. Introduction

Inverse potential field problems arise in geophysics when one wants to reconstruct density and/or magnetic source distributions from measured data and, like many other inverse problems, they are inherently difficult to solve because they are ill-posed.<sup>9</sup> Specifically they may fail to have a unique solution, and the solution may be extremely sensitive to errors.

In a general framework these difficulties are due to certain kinds of ambiguity in the inverse problem. In this paper we discuss the different kinds of ambiguity and how they are related to the solution of the problem. Hence we need to define precisely what we mean by "ambiguity."

In connection with a linear problem, ambiguity means that the solution to the problem is not unique. This, in turn, happens when the operator has a non-trivial null space. In

particular, we have ambiguity in a linear system of equations if it is under-determined or if the coefficient matrix is rank deficient.

In addition to this strict mathematical meaning, we will also use the word ‘‘ambiguity’’ when referring to components of the solution that cannot be recovered due to errors and noise, i.e., components that are practically undetermined. In other words, errors and noise also lead to ambiguity in the inverse problem, but this kind of ambiguity depends on both the characteristics of the problem and on the amount of noise in the data.

In this paper we demonstrate that a fundamental understanding of these two aspects of ambiguity is crucial for the practical solution of the potential-field inverse problem.

## 2. The Potential Field Problem

Our basis for solving the potential field problem is the inverse theory which was introduced to the geophysical community by Backus and Gilbert<sup>1,2</sup> and Parker.<sup>9</sup> In this setting, the source distribution is described by a continuous function  $f$  inside a source volume  $\Omega$ , and the relation between  $f$  and the field  $g$  outside  $\Omega$  is described by the forward model

$$(1) \quad \int_{\Omega} \mathcal{K}(\mathbf{r}, \mathbf{r}_o) f(\mathbf{r}) d\mathbf{r}^3 = g(\mathbf{r}_o).$$

Here,  $\mathbf{r} \in \Omega$  denotes a point inside the source volume, and  $\mathbf{r}_o$  denotes an observation point outside  $\Omega$ . The function  $\mathcal{K}$  is Green’s function for the gravitational or magnetic sources. This is a first-kind Fredholm equation for  $f$  which, of course, is an ill-posed problem.

It is well known that the inverse potential field problem in the form of (1) may have an ambiguous solution. There are (at least) two kinds of this inherent ambiguity. One kind of ambiguity is due to Green’s third identity;<sup>3</sup> if one allows the domain  $\Omega$  to be infinite, then any field  $g$  outside  $\Omega$  can be produced by both a source distribution inside  $\Omega$  and an infinitely thin layer of sources at the surface of  $\Omega$ . Another kind of ambiguity arises when the integral operator has a nontrivial null space, and the component of  $f$  in this null space is called the annihilator.<sup>9</sup> To overcome these ambiguity problems in the continuous formulation (1) one must incorporate prior knowledge about the solution into the solution process, leading to various forms of regularization algorithms for solving (1). In this functional analysis setting, the role of regularization is to remove the ambiguity

## 3. The Discretized Problem

In order to solve the potential field problem with real data, we must discretize the continuous problem (1) and represent the solution  $f$  by a finite amount of information. This can, of course, be done in many ways; here we use a discretization where the solution is approximated by a piecewise continuous function. Specifically we assume  $\Omega$  to be a box which is divided into a 3D grid of cells or prisms, and in each cell the solution is assumed to be constant. This leads to a system of linear equations

$$(1) \quad \mathbf{A} \mathbf{m} = \mathbf{b}$$

in which the right-hand side  $\mathbf{b}$  consists of the measured data, which we can consider as noisy samples of the continuous field  $g$ . The solution vector  $\mathbf{m}$  consists of the values of the

piecewise continuous solution in each cell. Finally, the coefficient matrix  $\mathbf{A}$  has elements given by

$$(2) \quad \mathbf{A}_{ij} = \int_{\Omega_j} K(\mathbf{r}, \mathbf{r}_{o,i}) d\mathbf{r}^3,$$

where  $\Omega_j$  denotes the  $j$ th cell and  $\mathbf{r}_{o,i}$  is the  $i$ th data point. The matrix  $\mathbf{A}$  has dimensions  $M \times N$ , where  $M$  is the number of measurements and  $N$  is the number of cells.

Any discretization of a linear inverse problem (1) can be considered as having a regularizing effect on the solution. The effect of the discretization can be considered as a projection of the infinite-dimensional problem onto a finite-dimensional one, and hence the discretization process is sometimes referred to as “regularization by projection.”<sup>4</sup>

However, in most applications the coefficient matrix  $\mathbf{A}$  will have a very large condition number, meaning that the discrete solution  $\mathbf{m}$  is very sensitive to perturbations. Hence, in any application with noisy data the regularization-by-projection does not provide enough stabilization to allow the computation of a useful solution. Data noise, as well as model errors and rounding errors, are amplified by the large condition number, and calls for additional stabilization in order to filter these contributions to the solution.

Whenever we face a linear system of the form (1) we encounter an *algebraic ambiguity* when the system is under-determined, i.e., when  $M < N$  (less data than unknowns). In this situation, the matrix has a non-trivial null space, and any component of the solution in this null space cannot be determined. It is therefore common to compute the minimum-norm solution, which is unique because the null-space component is zero. However, as demonstrated in Ref. 6, these minimum-norm solutions are not useful because they lack the ability to provide depth resolution.

Square or over-determined systems may or may not have ambiguous solutions, depending on the rank of the coefficient matrix. Our experience shows that if we choose the discretization parameters such that the matrix is square or over-determined, then – except for contrived cases – the matrix has full rank and the (least squares) solution is, in principle, unique. In practice, rounding errors often prevent us from computing a unique solution, but it is still important to keep in mind that square and over-determined systems usually lack the algebraic ambiguity. Of course, even with a full-rank matrix, the noise is likely to make the unique (least squares) solution useless.

#### 4. Depth Resolution

In order to discuss the potential for computing reconstructions with depth information, we first consider solutions to noise-free problems. Does the solution to a noise-free problem carry depth information, and how much? Recall that data can be considered as coming from a field  $g$  which is caused by a continuous distribution of sources  $f$  (in the real world), while the model consists of a grid of prisms with constant density or magnetization. We are obviously not able to capture all details of the function  $f$  in the model and in particular there is no guarantee that deep sources are well recovered.

Again, our experience shows that square and over-determined systems do provide depth information. We are not able to prove this, but we can justify that a full-rank matrix is able to provide the potential for depth resolution. Our tool is the singular value decompo-

sition (SVD) of the coefficient matrix:

$$(1) \quad \mathbf{A} = \mathbf{U} \mathbf{\Sigma} \mathbf{V}^T = \sum_{i=1}^{\min(M,N)} \mathbf{u}_i \sigma_i \mathbf{v}_i^T.$$

Here,  $\mathbf{U} = (\mathbf{u}_1, \dots, \mathbf{u}_M)$  and  $\mathbf{V} = (\mathbf{v}_1, \dots, \mathbf{v}_N)$  are orthogonal matrices of dimensions  $M \times M$  and  $N \times N$ , respectively, while  $\mathbf{\Sigma}$  is a diagonal matrix with nonzero elements  $\sigma_1 \geq \sigma_2 \geq \dots \geq \sigma_{\min(M,N)}$  along its main diagonal.

For a matrix with full column rank,  $\text{rank}(\mathbf{A}) = N \leq M$ , the complete set of columns  $\mathbf{v}_i$  of the right singular matrix  $\mathbf{V}$  are the basis vectors for the (least squares) solution. Since they form a basis for the space  $\mathbb{R}^N$  they can – in principle – represent any solution  $\mathbf{m}$ . In an orthogonal matrix it is impossible to have a row solely with elements that are small in magnitude. And since each row in the orthogonal matrix  $\mathbf{V}$  corresponds to a cell in the 3D solution grid, we are ensured that for each cell there is at least one column of  $\mathbf{V}$  with a non-negligible element corresponding to this column. Hence, the complete set of basis vectors must provide potential depth resolution whenever there is no algebraic ambiguity.

On the other hand, if the matrix is under-determined and we compute the minimum-norm solution, then we only make use of a subset of the right singular vectors, and there is no guarantee that each cell will have at least one non-negligible element in this set of vectors. Hence, there is no guarantee for depth resolution in the minimum-norm solution to under-determined problems, and these solutions usually lack any depth resolution.<sup>5</sup>

The tool for analyzing the potential for depth resolution in a given system is the Depth Resolution Plot (**DRP**).<sup>6</sup> For each singular vector  $\mathbf{v}_i$ , the DRP shows the magnitude of the elements that corresponds to the cells in each layer of the grid, i.e., it indicates the depth information in all singular vectors that can potentially take part in the reconstruction. In this way we can immediately see which singular vectors are needed to reconstruct features at a certain depth. We stress that the information in this plot comes solely from the coefficient matrix; it does not depend on the measurements. Note that the singular vectors, and hence also the DRP, have no physical units.

Figure 1a shows an example of a DRP for a magnetic test problem whose source volume  $\Omega$  is a box of dimensions  $1500 \times 1500 \times 600 \text{ m}^3$ . Our discretization uses a  $13 \times 13 \times 13$  grid, i.e., the solution consists of  $N = 13^3 = 2197$  cells. Moreover, we use  $M = 3600$  data points arranged in a  $60 \times 60$  grid, covering an area of  $1500 \times 1500 \text{ m}^2$ , and located 10 m above the source volume. We assume here that the direction of the inducing field is vertical, i.e., having an inclination of  $90^\circ$  and a declination of  $0^\circ$ .

## 5. Regularization and Depth Resolution

We now turn to the issue of the ambiguity due to noise, and in particular the limitations to depth resolution due to the errors in the data  $\mathbf{b}$ . For simplicity we ignore any errors in the positions of the data points, and consider only noise in the data coming from inaccuracies in the measurements.

Whenever noise is present, we must use regularization to reduce the solution's sensitivity to the noise. The effect of the regularization is, effectively, to filter the noise and dampen those components in the regularized solution that are most sensitive to the noise. Hence we must determine how to identify and separate the reliable components from the noisy ones. The most convenient tool for this analysis is the Discrete Picard Plot (**DPP**).<sup>7</sup>

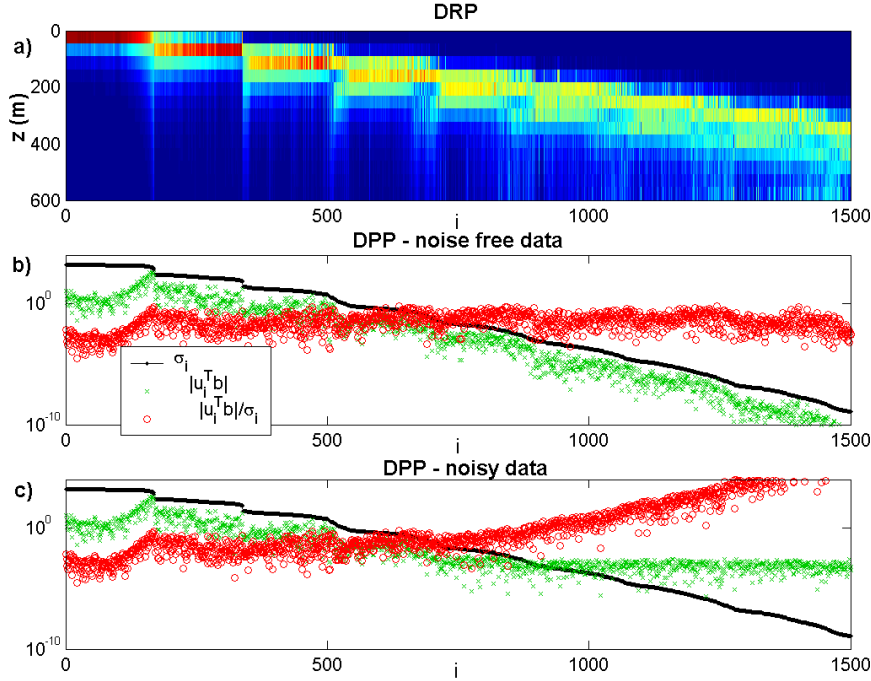


Fig. 1. a) Depth Resolution Plot (DRP) for a test problem with  $M = 3600$  and  $N = 2197$ . See text for details. Only the first 1500 SVD components are shown. b) Discrete Picard Plot (DPP) for the same source volume containing a prismatic body source with unit magnetization. Note that the data are noise free. c) DPP for the same problem but with noisy data, with noise level  $\eta_{\text{noise}} = 10^{-3}$ .

Similar to the DRP, the DPP requires the SVD of the coefficient matrix. We recall that the (least squares) solution to a square or over-determined problem (1) can be expressed in terms of the SVD as

$$(1) \quad \mathbf{m} = \sum_{i=1}^{\min(M,N)} \frac{\mathbf{u}_i^T \mathbf{b}}{\sigma_i} \mathbf{v}_i,$$

i.e., the right singular vectors  $\mathbf{v}_i$  are the basis vectors for the solution, and the quantities  $\mathbf{u}_i^T \mathbf{b}/\sigma_i$  are the expansion coefficients. The DPP is a plot of the quantities  $|\mathbf{u}_i^T \mathbf{b}|$ ,  $\sigma_i$  and  $|\mathbf{u}_i^T \mathbf{b}|/\sigma_i$ , and it shows all the information necessary to understand how noise enters. In particular we know that the SVD coefficients  $|\mathbf{u}_i^T \mathbf{b}|$  will decay, on the average, until they level off at a plateau determined by the noise in the data, while the initial decaying SVD coefficients are dominated by noise-free data.<sup>7,8</sup> The choice of filtering to apply in order to obtain reliable solutions will depend on the amount of noise  $\mathbf{e}$  in the data, given by  $\mathbf{b} = \mathbf{b}_{\text{pure}} + \mathbf{e}$ . If the noise in each measurement is additive and has a standard deviation  $\eta_{\text{noise}}$ , then

$$(2) \quad \begin{aligned} |\mathbf{u}_i^T \mathbf{b}| &= |\mathbf{u}_i^T \mathbf{b}_{\text{pure}} + \mathbf{u}_i^T \mathbf{e}| \\ &\approx \max \{ |\mathbf{u}_i^T \mathbf{b}_{\text{pure}}|, |\mathbf{u}_i^T \mathbf{e}| \} \\ &\approx \max \{ |\mathbf{u}_i^T \mathbf{b}_{\text{pure}}|, \eta_{\text{noise}} \}. \end{aligned}$$

Hence, the right-hand side coefficients  $|\mathbf{u}_i^T \mathbf{b}|$  for which  $|\mathbf{u}_i^T \mathbf{b}_{\text{pure}}| > \eta_{\text{noise}}$  are dominated by the pure field, while coefficients with  $|\mathbf{u}_i^T \mathbf{b}_{\text{pure}}| < \eta_{\text{noise}}$  are dominated by noise. Consequently, the solution coefficients  $|\mathbf{u}_i^T \mathbf{b}|/\sigma_i$  associated with the small singular values are approximately  $\eta_{\text{noise}}/\sigma_i$ , i.e., they are dominated by noise.

Figures 1b and 1c show two examples of DPP for noise free and noisy data, respectively. The noise level is  $\eta_{\text{noise}} = 10^{-3}$ . The examples use the source volume from Section 4, containing a prismatic source model with unit magnetization. The prismatic body has cell coordinates 5–7 along the  $x$ -direction, 4–6 along the  $y$ -direction, and 5–6 along the  $z$ -direction. We also assume that the direction of magnetization of the source model is parallel to the direction of the inducing field and that both directions are vertical.

The analysis of Figs. 1b–c shows how a visual inspection of the DPP will immediately give the required insight about which SVD components in the solution are reliable, and which must be filtered out. The SVD components that are dominated by the noise (located at the plateau in the DPP) correspond to components in the solution that are practically undetermined – they cannot be recovered from the given data. For this reason we can also talk about the *noise ambiguity* due to the noisy data. Due to this noise ambiguity, discretizations of inverse potential field problems are practically under-determined – also when  $M \geq N$ . To deal with noise ambiguity we apply regularization, whose effect – as mentioned above – is to remove or filter the undesired components in the regularized solution. A quite general approach to regularization is to solve the following minimization problem

$$(3) \quad \min_{\mathbf{m}} \{ \|\mathbf{A} \mathbf{m} - \mathbf{b}\|_2^2 + \Gamma(\mathbf{m}) \},$$

which is often referred to as Tikhonov regularization. The second term  $\Gamma(\mathbf{m})$  is called the stabilizer, and its role is to provide the desired filter. In this work, for simplicity we consider only the simple choice  $\Gamma(\mathbf{m}) = \|\mathbf{m}\|_2^2$ .

One way to understand how much depth resolution can be obtained with given noisy data is to compare the information in the DRP and DPP. Specifically, the DPP shows how many SVD components can be recovered, while the DRP shows how much depth information is available in the corresponding set of singular vectors  $\mathbf{v}_i$ . Figure 1 illustrates this point, while Table 1 summarizes our analysis. We emphasize again that it is the combined inspection of the DRP and DPP that reveals how much depth resolution can be achieved in a given discretized problem and with a given noise-level in the data. The DPP reveals how many SVD components can be included in the regularized solution, and the DRP shows how much depth resolution can be achieved with these SVD components.

## 6. Example

To illustrate the issues discussed above we consider here an inverse test problem using the same source volume  $\Omega$  as in Section 4, i.e., a volume divided into a  $13 \times 13 \times 13$  grid of cells, covering a horizontal area of  $1500 \times 1500 \text{ m}^2$  and with depth ranging from 0 to 600 m. The volume contains a prismatic source model with unit magnetization and with cell coordinates 5–7 along the  $x$ -direction, 4–6 along the  $y$ -direction, and 4–5 along the  $z$ -direction. Again, we assume that the direction of both the source model and the inducing field are vertical. Figure 2 illustrates the source model used for generating the test data.

In our solution procedure we want to avoid committing “inverse crime,” i.e., using a model which resembles the true solution too much. Therefore the grid used for reconstructing the source distribution is made of  $15 \times 15 \times 15$  cells covering the same source volume  $\Omega$ . In other words: we use slightly different grids for generating the synthetic data, and for reconstructing the solution. This simulates the real-world situation where there is

Table 1. Overview of ambiguities and depth resolution issues in inverse potential field problems.

CONTINUOUS PROBLEM	
$\mathcal{K} f = g$	
<i>Inherent ambiguities</i>	
DISCRETIZED PROBLEM	
$\mathbf{A} \mathbf{m} = \mathbf{b}$	
<i>Algebraic ambiguity</i> when the system is under-determined	<i>Noise ambiguity</i> due to ill-conditioning of $\mathbf{A}$ and due to noise in the data $\mathbf{b}$
Analysis tool: <u>DRP</u>	Analysis tool: <u>DPP</u>
Shows the potential depth resolution in the matrix $\mathbf{A}$	Shows the reliable and the noisy SVD-components in the data $\mathbf{b}$
Combined inspection of <u>DRP</u> and <u>DPP</u> shows the achievable depth resolution for a given noisy problem	

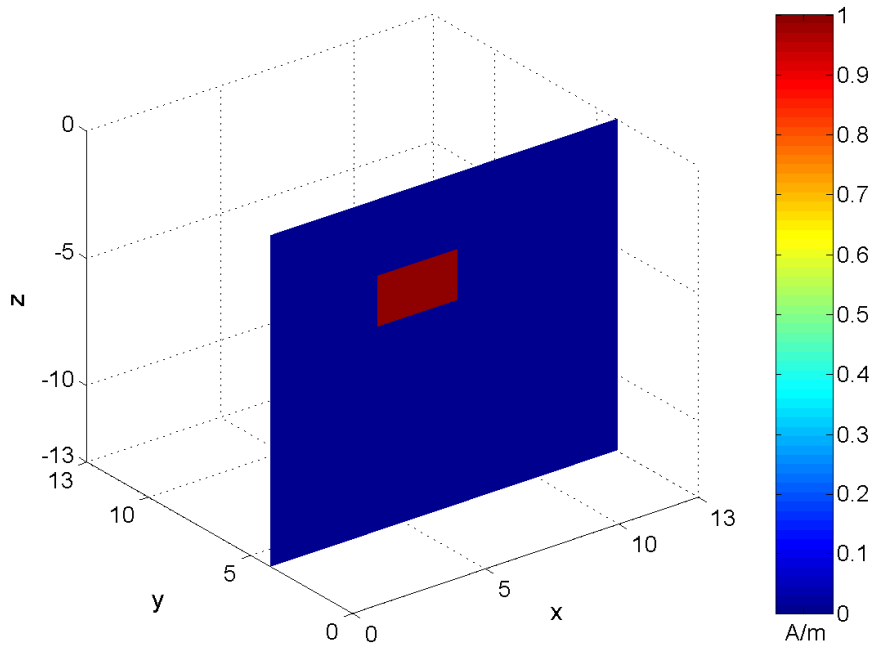


Fig. 1. Source model used for generating the test data. The source volume is divided into a  $13 \times 13 \times 13$  grid of cells, covering a horizontal area of  $1500 \times 1500 \text{ m}^2$  and with depth ranging from 0 to 600 m. Note that the numbers along the  $x$ ,  $y$ , and  $z$  axes represent the number of cells in the grid. The source model has a unit magnetization and cell coordinates 5–7 along the  $x$ -direction, 4–6 along the  $y$ -direction, and 4–5 along the  $z$ -direction.

no resemblance between the discretization grid and the real distribution of magnetization in the nature.

The DRP and DPP for this  $15 \times 15 \times 15$  reconstruction grid (using the data created by the  $13 \times 13 \times 13$  forward problem) are shown in Fig. 3. As we can see from the DPP, the fact that the data was generated using a discretization different from that used for solving

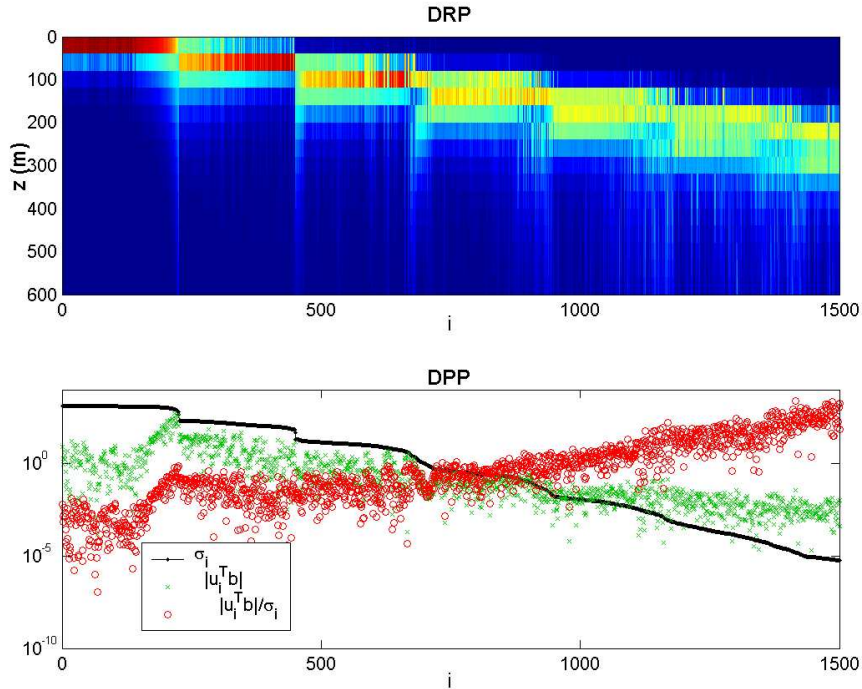


Fig. 2. Depth Resolution Plot and Discrete Picard Plot for the considered inverse test problem. Note that the grid used for reconstructing the source distribution is made of  $15 \times 15 \times 15$  cells covering the same source volume of Fig. 2. Only the first 1500 SVD components are shown. As we can see, the use of different discretizations in the forward and inverse problems introduces errors that manifest for  $i > 900$ .

the inverse problem introduces some errors, that manifest themselves for  $i > 900$ . Note that this situation is very similar to the one shown in Fig. 1c with white noise added. Therefore we must filter out the solution components for  $i > 900$ .

Looking now at the DRP in Fig. 3, we see that for  $i < 900$  the elements of the DRP with large magnitude are placed solely in the top 5 layers, corresponding to a depth of about 200 m. Hence we can conclude that the inclusion of 900 SVD components in the reconstruction corresponds to a depth resolution of about 200 m.

The solution obtained with 900 SVD components is shown in Fig. 4. Despite the grids used for the forward and the inverse problems being different, a good reconstruction of the source can be obtained provided that the algebraic ambiguity is kept low. The figure also confirms our conclusion from the DRP, namely, that there is no depth resolution below a depth of about 200 m.

Note that when a finer discretization is used, the error caused by the use of different discretizations in the forward and inverse problems becomes more and more negligible, allowing a better depth resolution.

## 7. Concluding Remarks

We discussed the implications of the algebraic and noise ambiguities in inverse potential field problems, and demonstrated how these ambiguities can be studied by means of the Depth Resolution Plot and the Discrete Picard Plot. We also demonstrated how the combined inspection of these two plots leads to a better understanding of how much depth resolution that can be achieved in a reconstruction from noisy data. The two

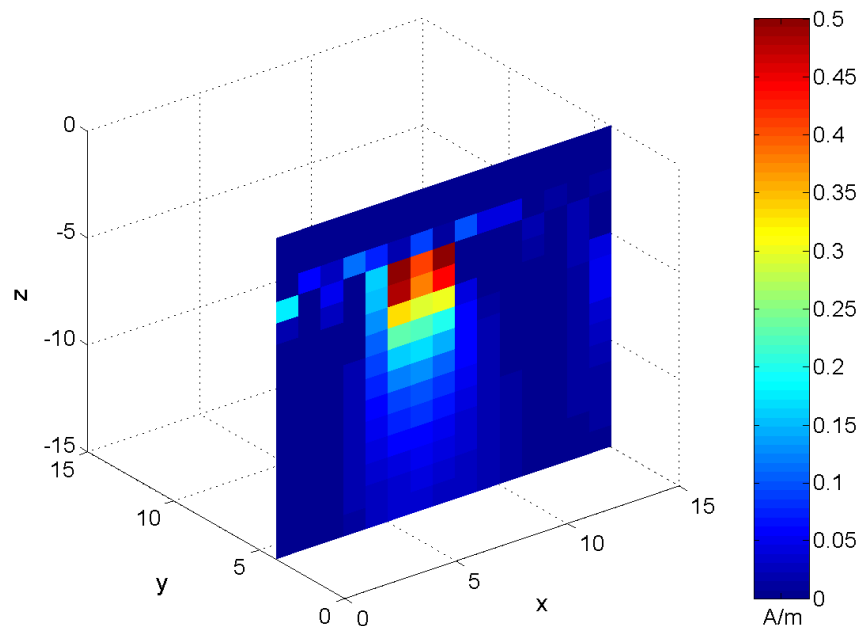


Fig. 3. Reconstructed solution obtained using 900 SVD components. The source volume is divided into a  $15 \times 15 \times 15$  grid of cells, covering a horizontal area of  $1500 \times 1500 \text{ m}^2$  and with depth ranging from 0 to 600 m. Note that the numbers along the  $x$ ,  $y$ , and  $z$  axes represent the number of cells in the grid.

plots require the computation of the SVD, and we are currently investigating large-scale methods for producing these plots without the need for the SVD. Finally we provided a numerical example which shows that some depth resolution is possible with noisy data, when using square or over-determined systems of equations.

## REFERENCES

1. G. Backus and F. Gilbert, *The resolving power of gross earth data*, Geophys. J. Roy. Astron. Soc., 16, 169–205, 1968.
2. G. Backus and F. Gilbert, *Uniqueness in the inversion of inaccurate gross earth data*, Phil. Trans. Roy. Soc. London, Ser. A, 266, 123–192, 1970.
3. R. J. Blakely, *Potential Theory in Gravity and Magnetic Applications*, Cambridge University Press, 1996.
4. H. W. Engl, M. Hanke and A. Neubauer, *Regularization of Inverse Problems*, Kluwer Academic Publishers, Dordrecht, 1996.
5. M. Fedi and A. Rapolla, *3-D inversion of gravity and magnetic data with depth resolution*, Geophysics, 64, 452–460, 1999.
6. M. Fedi, P. C. Hansen and V. Paoletti, *Tutorial: Analysis of depth resolution in potential-field inversion*, Geophysics, 70, A1–A11, 2005.
7. P. C. Hansen, *The discrete Picard condition for discrete ill-posed problems*, BIT, 30, 658–672, 1990.
8. P. C. Hansen, *Rank-Deficient and Discrete Ill-Posed Problems*, SIAM, Philadelphia, 1998.
9. R. L. Parker, *Understanding inverse theory*, Ann. Rev. Earth Planet. Sci., 5, 35–64, 1989.